Survey of Geosynchronous Satellite Polarization Signatures

Blake C. Eastman, Audra M. Jensen, Daniel S. O'Keefe, Francis K. Chun
Department of Physics and Meteorology, US Air Force Academy, USAF Academy, CO
David M. Strong
Strong EO Imaging, Inc., Colorado Springs, CO 80908

ABSTRACT

Maintaining Space Situational Awareness requires the capability to identify and characterize orbiting satellites. One photometric technique available to extract information from unresolved satellite images is polarimetry. To explore the information potentially provided by satellite polarization signatures, various geosynchronous satellites are measured using a polarimeter over the course of several years. The polarimeter consists of a CCD camera behind four polarization filters on a rotating filter wheel, mounted to a 16-inch f/8.2 Cassegrain telescope. Review of the signatures obtained suggests that polarized light from satellites is generally from solar panels outside a glint, and the payload of the satellite during a glint.

1. INTRODUCTION

Space Situational Awareness (SSA) is becoming increasingly important as space becomes more contested and congested. Armed Forces doctrine identifies SSA as the "knowledge and characterization of space objects and the [operational environment] upon which space operations depend" [1]. Critical to maintaining SSA, then, is the ability to identify and characterize orbiting satellites, a form of space object possessing capabilities which influence the space operational environment.

Unfortunately, optical characterization of satellites is seldom as simple as taking a picture through a telescope. At orbital distances from the ground, a satellite must either be abnormally large, or the telescope used to observe it must possess an unreasonably large aperture for a resolved image to be acquired. As such, SSA requires the employment of techniques to extract information from unresolved images. Historically, this has been achieved using photometry [2-4]. Photometry has revealed that observations of unresolved images across nights can yield consistent data [5] and confirmed that satellite glints are caused by solar panels [6].

Polarimetry is another technique which shows promise in SSA applications. Other photometric techniques attempt to discern information about targets by collecting color data. While the frequency of reflected light (color) is useful, polarimetry offers an opportunity to study another aspect of the reflected light – its orientation. The polarization of reflected light is governed by different phenomena than the color, offering different insights into the surfaces from which the light is reflected. Specifically, it is possible to collect information about the polarization of satellite light by taking near-simultaneous images of the intensity of light at four different orientations. [7]

For this project, the polarization signatures of several geosynchronous satellites are measured across several years. The process used to convert raw polarimeter data into a useable polarization signature is presented. Features consistent with the polarization of solar panel reflections are identified and reviewed. Further, evidence of payload or satellite bus influence on the polarization signature of satellites is also displayed. These influences give insight into the information provided by utilizing polarimetry for SSA purposes.

2. INSTRUMENTATION AND PROCESSING

A 16-inch aperture f/8.2 Cassegrain telescope is used to collect light for observations. Images are taken using an Andor Ulta U47 CCD camera. Light collected from the telescope is passed through one of four polarization filters before being imaged, filtering light at either 0°, 45°, 90°, or 135° with respect to the focal plane of the camera. Only one filter is used at a time, and the filters are rotated at variable intervals depending on the intensity of the satellite reflection.

The strength of the signal at each orientation is determined through aperture photometry. The total counts at each pixel of the camera over the satellite are summed, and the background is removed. The result is a measurement of the total photons detected by the camera.

Each orientation is measured near-simultaneously. Thus, it is reasonable to approximate each measurement as simultaneous. With this approximation, it is possible to convert the counts at each orientation into corresponding Stokes parameters, which quantify the relationships between the intensity of light at different orientations. The first three stokes parameters, S_0, S_1, and S_2 give the total intensity of the light, the difference in intensity between the zero- and 90-degree angles, and the difference in intensity between the 45- and 135-degree angles respectively [8].

Atmospheric influences have the potential to disrupt the polarization signal from the satellite. To detect these signals, the correlation of the polarization of two satellites in the same image frame can be considered. High The above equations are useful when considering the intensity of light measured by an ideal polarimeter; however, optical influences by the telescope and polarization films can cause aberrations from the true polarization of the source. To correct for this issue, the polarimeter is calibrated by placing a polarimeter and polarization generator in front of the optical system, measuring the polarization at known angles using the polarimeter. This information is compiled into a calibration matrix, permitting accurate determination of the polarization of a given signal [9]. The accuracy of the polarimeter can be verified by observing known polarization stars.
correlation suggests the atmosphere is primarily responsible for the observed polarization – as it is causing uniform shifts in polarization throughout the image [10].

The Stokes parameters serve as an intermediary quantification of the polarized signal. It is more useful to consider the degree of linear polarization (DOLP) and angle of linear polarization (AOLP), which describe how much light is polarized and the orientation of that polarized light respectively [8].

$$DOLP = \frac{\sqrt{s_1^2 + s_2^2}}{S_0}$$

$$AOLP = \frac{1}{2}(\arctan S_2/S_1)$$

These are the measures of polarization utilized to view and understand the polarization of observed satellites.

3. RESULTS

Polarization data for several satellites across several nights of observation is available, as provided in table 1. The characteristics of the observed satellites are also available in table 2. To compare observations over different nights and between different satellites, it is necessary to understand the polarization signal in the context of the geometry between the satellite and the sun. To do so, the Longitudinal Phase Angle (LPA) of the satellite is utilized to understand the polarization of a satellite at different points in observation. The LPA is the projection of the solar phase angle onto the equatorial plane. It reaches zero when the solar phase angle is at a minimum.

Table 1: List of all satellites observed, their launch dates, as well as associated dates of observation. Observations with corrupted data (due to atmospheric conditions) are not included.

Satellite	Launch Date	Observations
DTV10	07 Jul 2007	23 Feb 2021 16 Oct 2021 20 Feb 2022
DTV12	29 Dec 2009	23 Feb 2021 16 Oct 2021 20 Feb 2022
DTV15	27 May 2015	16 Oct 2021 20 Feb 2022
SES3	15 Jul 2011	22 Oct 2021
XM4	30 Oct 2006	29 Oct 2021
MEXSAT3	19 Dec 2012	30 Oct 2021

Table 2: List of the characteristics (bus configuration, mass, and payload equipment) of the observed satellites [11].

Satellite	Bus	Mass	Equipment
DTV10	BSS-702	5893 kg	32 (+12) Ka-band transponders, 55 (+15) Ka-band Spot-Beam transponders
DTV12	BSS-702	5893 kg	32 (+12) Ka-band transponders, 55 (+15) Ka-band Spot-Beam transponders
DTV15	Eurostar-3000	6205 kg	30 high power Ku-band transponders, 24 Ka-band transponders, 18 Reverse Band transponders
SES 3	STAR-2	3170 kg	24 active C-band, 24 Ku-band and 2 Ka-band transponders
XM4	BSS-702	5193 kg	13.3 kW Digital Audio Radio, 2 active S-band transponders, each w/16 active (6 spare) 228 W TWT
MEXSAT3	STAR-2	3050 kg	12 C-band and 12 Ku-band transponders

A common feature among these observations of polarization signatures is a higher DOLP from satellites at larger LPA. In Fig. 1., a sample of four different satellite observations is included. By viewing the red trace, one can see DOLP reaches a minimum around zero LPA, whereas it is at its highest point near the beginning or end of the observation, when the satellite is at its highest absolute LPA observed. Not only does DOLP appear to follow a consistent pattern among satellites, but a common change occurs in AOLP when the satellite crosses zero LPA. With LPA less than zero, the satellites have an AOLP between -90º and -60º, whereas with LPA greater than zero, they have an AOLP between 60º and 90º.

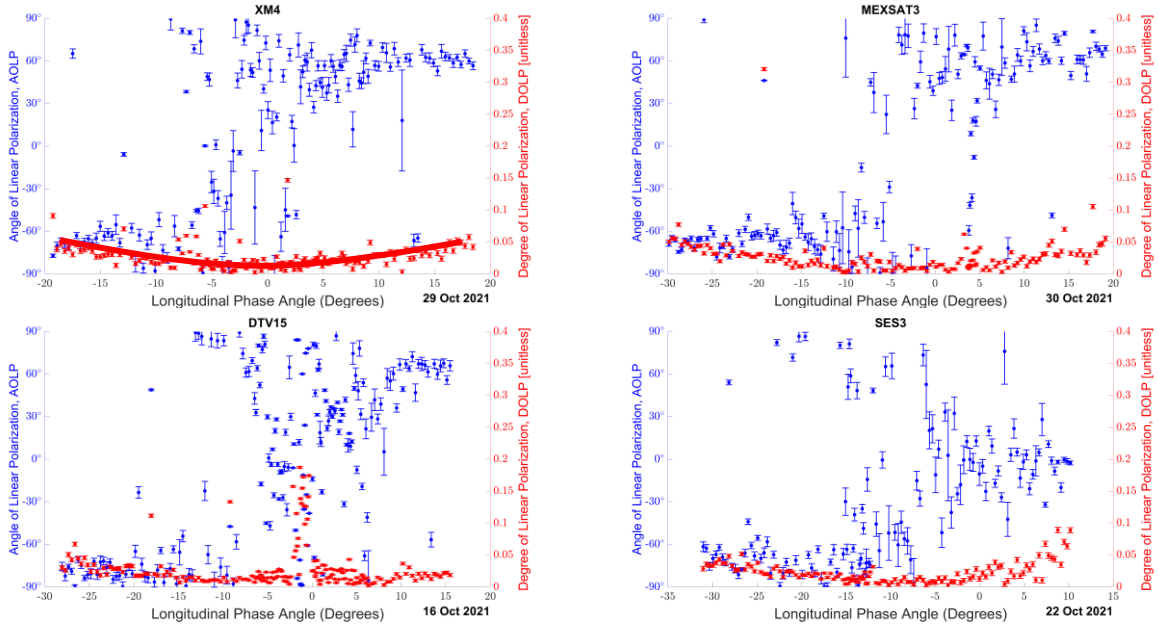

Fig. 1. Polarization signatures for satellites on different nights. The blue trace on the left axis shows the AOLP, while the red trace on the right axis shows the DOLP. Notable features common to all signatures include a change in average polarization angle when the satellite crosses zero LPA, as well as higher degrees of linear polarization at higher LPAs. The identified trend in DOLP is depicted in the plot of XM4 by a red curve.

Solar panels have been observed to follow a similar pattern, having higher DOLP when viewed from higher phase angles. Similarly, a distinct shift in AOLP as phase angle shifts through zero has also been observed. These observations are depicted in Fig. 2. As the baseline DOLP and AOLP of satellites behave in the same manner, it is likely the solar panels of each satellite are responsible for creating the observed baseline polarization signatures.

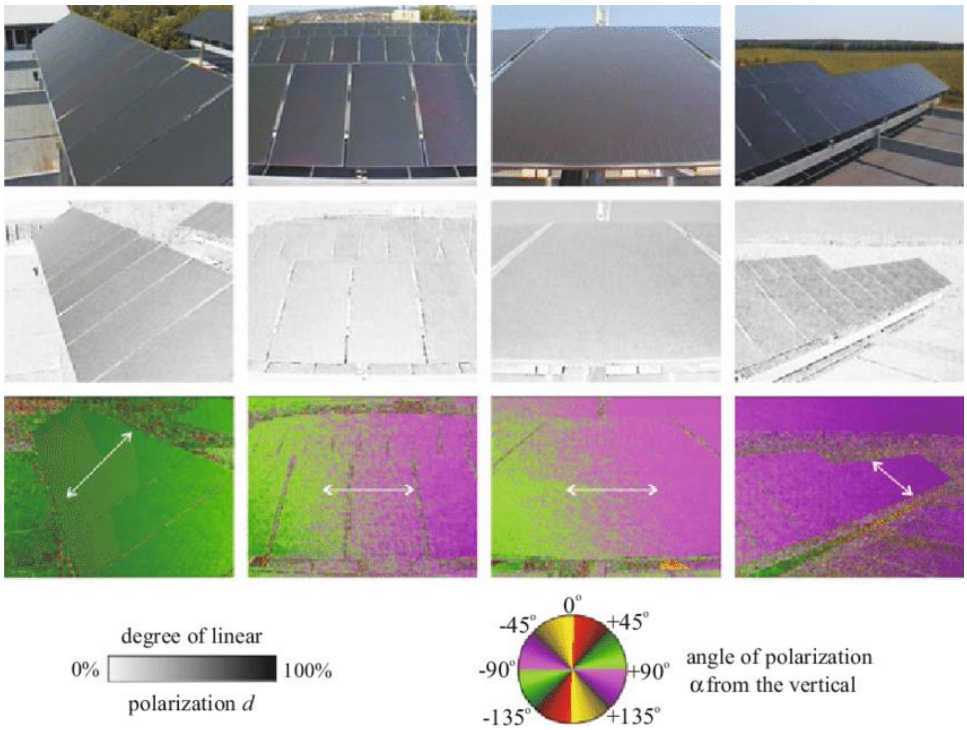

Fig. 2. Resolved images of solar panels at various angles [12]. The top row shows the solar panels in visible light, the middle shows the DOLP of the solar panels, while the bottom shows the AOLP from the vertical axis of the camera.

These results are further confirmed by looking at the reflectance properties of silicon. When restricting the view of reflectance to the plane in which the incident and reflected rays interact with the material one can distinguish light by the orientation of its electric field. Light with its electric field oriented in the plane of reflection is referred to as p-polarized light and is more likely to be refracted. Light with its electric field oriented perpendicular to the plane of reflection is referred to as s-polarized light and is more likely to be reflected, see Fig. 3.

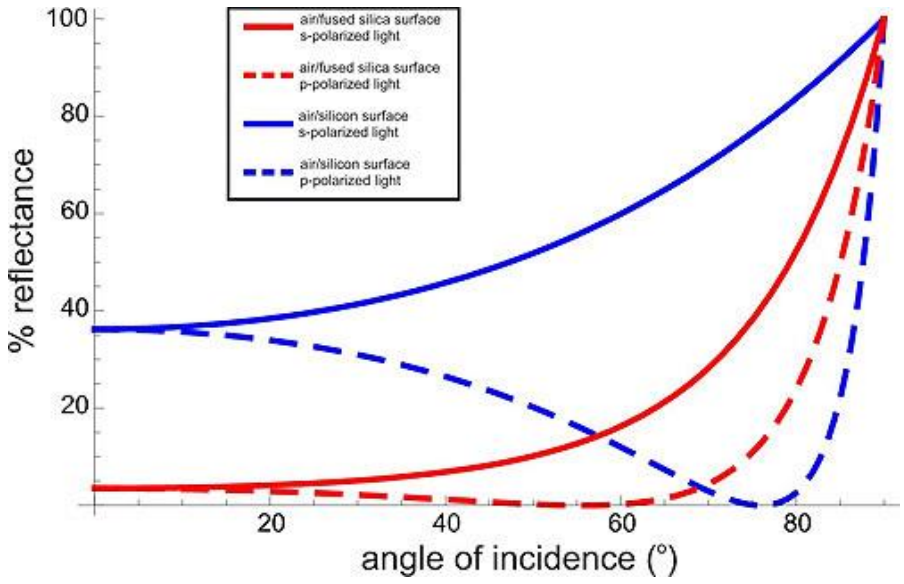

Fig. 3. The graph shows that at Brewster's angle (shown here for an air-fused silica interface, about 55 degrees and about 77 degrees for an air-silicon interface), none of the p-polarized light is reflected [13].

Since the index of refraction of air is very similar to that of space, the plots for a solar panel in space should be nearly identical to those shown in the Figure. At a zero angle of incidence, the amount of s and p-polarized light reflected is the same so DOLP is zero as well. The Brewster's angle is where the maximum DOLP should occur for the reflected light from the materials surface. So, if most of the light is reflected from the solar panels of the satellite, one should observe a maximum DOLP near the Brewster's angle and a DOLP near zero at a zero angle of incidence.

Interestingly, not all satellites achieve minimum baseline DOLP around an LPA of zero degrees. In Fig. 4., the minimum is achieved before the satellite reaches that point in its orbit. However, not all satellites maintain solar panels in the same orientation. By viewing the intensity of the reflected light from the satellite in Fig 4., it is evident that the viewing phase angle of the satellite solar panels reaches its minimum (corresponding with maximum intensity) along with the DOLP. This minimum also aligns with the transition in observed AOLP.

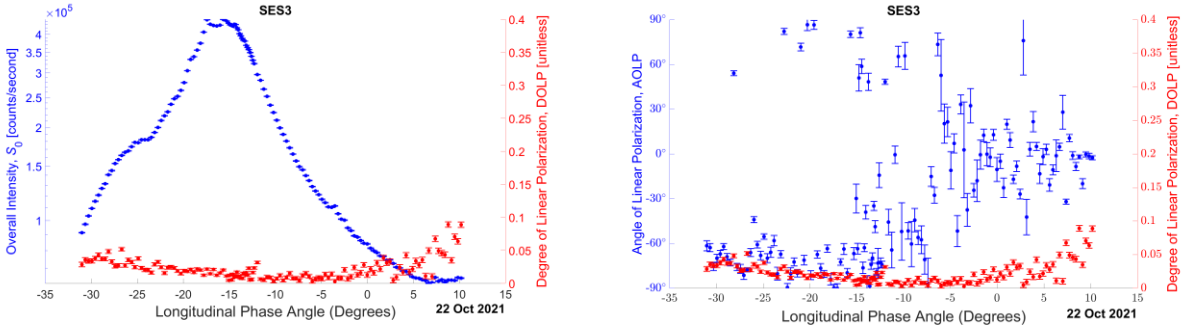

Fig. 4. A closer look at the polarization signature of SES3 on 22 October 2021, revealing the minimum DOLP occurs when the satellite is brightest.

Some observations see a distinct increase in DOLP while the satellite is near minimum LPA. This pattern in DOLP is not consistent with the polarization signature of solar panels. Thus, the source of this polarized signal must come from components of the satellite bus or payload. The polarization signature of DTV15 supports this, as it sees the largest increase in DOLP occur between two separate glints (likely caused by offset solar panels), suggesting the measured DOLP is not derived from the solar panel. This can be seen in Fig. 5.

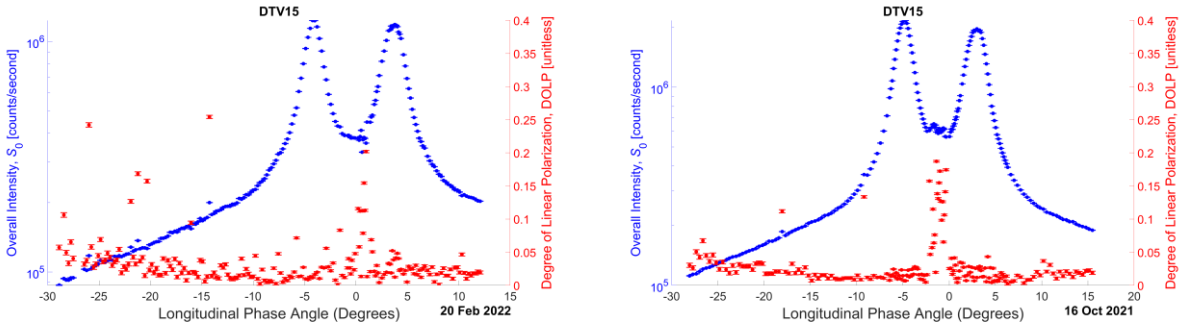

Fig. 5. The polarization signature of DTV15 on two different nights, revealing a distinctive double glint, as well as elevated DOLP occurring outside either glint.

Observations of DTV10 and DTV12 suggest that the configuration of the payload is a highly influential factor in the generation of the polarized signal during glint. Both satellites, having identical bus type and payload, demonstrate a consistently different character of polarization signal. Three nights of observation for these satellites are included in Fig. 6.

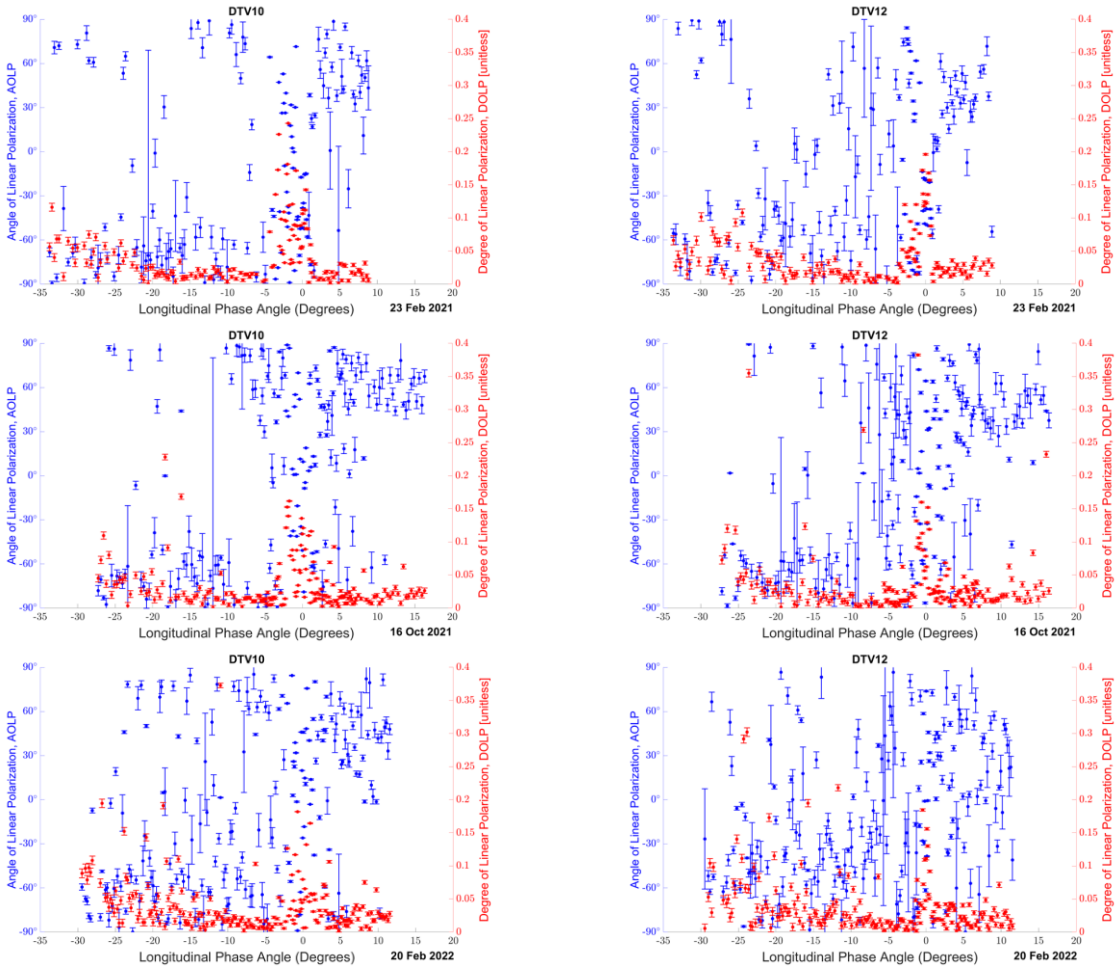

Fig. 6. A comparison of polarization signatures between DTV10 (left column) and DTV12 (right column) on three different nights.

Interestingly, the satellites maintain a consistent pattern in DOLP between nights. DTV12 has a sharp and short increase in DOLP, whereas DTV10 has a smoother and longer increase in DOLP. It is possible the cause of this

phenomenon is the orientation of each satellite's communications equipment. While both satellites are identical, they service different regions. As a result, the component of the satellites which causes this feature in DOLP is oriented in such a way that its signal is measured longer on DTV10 than on DTV12.

4. CONCLUSIONS

Satellite polarization signatures appear to possess a distinct and meaningful pattern; the influence of solar panels on the reflected light's polarization is identifiable in both DOLP and AOLP and polarization glints are consistent across nights of observation for the same satellite. Furthermore, differences between polarization signatures in identical satellites suggest that polarized light during a glint is influenced by the configuration of the payload. This hints at the potential utility offered by satellite polarization in determining the status of satellite payloads through unresolved imaging.

It remains challenging to discern specific details about a satellite from its polarization glint. Due to the small aperture size used to observe the satellites in this survey, the time between individual image captures heavily reduces the temporal resolution of the polarization during the glint. In the future, it may prove useful to observe satellites through larger aperture telescopes (such as a new 1-meter telescope installed at the United States Air Force Academy). This will permit a deeper understanding of the polarization signal during a glint, an important step in learning more about the satellite's payload and mission.

Another important step in utilizing polarimetry in SSA is collecting polarization signatures simultaneously from multiple ground sites. Observing a satellite at multiple angles offers an opportunity to learn more about the geometry involved in the generation of polarization signatures. Upgrades to the Air Force Academy operated Falcon Telescope Network will offer more ground-based polarimeters for use in SSA research, permitting a deeper understanding of the geometries involved.

5. ACKNOWLEDGEMENTS

We want to acknowledge the support of the Air Force Office of Scientific Research. Additionally, this paper is the result of multiple physics senior capstone projects and independent studies at the United States Air Force Academy.

6. REFERENCES

[1] Scott, K. D. (2018, April 10). Joint Publication 3-14. Space Operations. Chairman of the Joint Chiefs of Staff. Retrieved September 6, 2020

[2] Payne, T. E., Gregory, S. A., Houtkooper, N. M., and Burdullis, T. W., "Classification of Geosynchronous Satellites Using Photometric Techniques," Proceedings of the 2002 AMOS Technical Conference, The Maui Economic Development Board, Inc., Kihei, Maui, HI (2002).

[3] Payne, T. E., Gregory, S. A., and Luu, K., "SSA Analysis of GEOS Photometric Signature Classifications and Solar Panel Offsets," Proceedings of the 2006 AMOS Technical Conference, The Maui Economic Development Board, Inc., 667-673 (2006).

[4] Vrba, F.J., DiVittorio, M.E., Hindsley, R.B., Schmitt, H.R., Armstrong, J.T., Shankland, P.D., Hutter, D.J., and Benson, J.A., "A survey of geosynchronous satellite glints." The 2009 AMOS Technical Conference Proceedings, The Maui Economic Development Board, Inc., Kihei, Maui, HI (2009).

[5] Schildknecht, T., Vananti, A., Krag, H., and Erd, C., "Reflectance spectra of space debris in GEO," The 2009 AMOS Technical Conference Proceedings, The Maui Economic Development Board, Inc., Kihei, Maui, HI, 220-227 (2009).

[6] Dunsmore, A.N., J.A. Key, R.M. Tucker, E.M. Weld, F.K. Chun, and R.D. Tippets, "Spectral Measurements of Geosynchronous Satellites During Glint Season," J. Spacecraft and Rockets, (2016). doi: http://arc.aiaa.org/doi/abs/10.2514/1.A33583.

[7] Zimmerman, L.A., S.S. Chun, M.F. Pirozzoli, D.M. Strong, M.K. Plummer, and F.K. Chun, "Near-Simultaneous Polarization and Spectral Optical Measurements of Geosynchronous Satellites," The 2020 AMOS Technical Conference Proceedings, The Maui Economic Development Board, Inc., Kihei, Maui, HI, 2020

[8] Born, Max, and Emil Wolf. Principles of Optics: 60th Anniversary Edition. 7th ed., Cambridge University Press, 2019.

[9] Pirozzoli, M. F., Zimmerman, L. A., Korta, M., Scheppe, A. D., Jensen, A. M., Strong, D. M., Plummer, M. K., O'Keefe, D. S., & Chun, F. K. (2022). Calibration, sensitivity analysis, and demonstration of a basic polarimeter

for Artificial Satellite Observations. Advances in Space Research, 69(1), 581–591. https://doi.org/10.1016/j.asr.2021.10.003
[10] Jensen, A. M., Plummer, M. K., O'Keefe, D. S., Chun, F. K., & Strong, D. M. (2021). Observations of Satellites Using Near-Simultaneous Polarization Measurements.
[11] Krebs, G. Gunter's Space Page. Retrieved from Space.SkyRocket: https://space.skyrocket.de/index.html
[12] Horváth, G., Kriska, G., & Robertson, B. (2014). Anthropogenic polarization and polarized light pollution inducing polarized ecological traps. Polarized Light and Polarization Vision in Animal Sciences, 443–513. https://doi.org/10.1007/978-3-642-54718-8_20
[13] Michael C. Fink – thin film scientist, K. W. – astronomy product manager. (2008, December 11). The polarization of light by reflection. Photonics Media. Retrieved August 31, 2022, from https://www.photonics.com/Articles/The_Polarization_of_Light_by_Reflection/a35808

7. DISCLAIMER AND PUBLIC RELEASE STATEMENT

DISCLAIMER: The views expressed in this article are those of the authors and do not necessarily reflect the official policy or position of the United States Air Force Academy, the United States Air Force, the United States Space Force, the Department of Defense, or the U.S. Government.

DISTRIBUTION STATEMENT A: Approved for public release: distribution unlimited. PA#: USAFA-DF-2022-706